"REVIEWED"

APPLICATIONS OF THE CLARK MODEL TO WINTER STORMS OVER THE WASATCH PLATEAU

James A. Heimbach, Jr
University of North Carolina
Asheville, NC 28804

and

William D. Hall
National Center for Atmospheric Research
Boulder, CO 80307

Abstract. The configuration of the Clark mesoscale model to a field experiment conducted over the central Utah Wasatch Plateau experimental area is briefly described. Its application is demonstrated using one case from the early winter 1991 Utah/NOAA Cooperative Atmospheric Modification Research Program. Observations of sulfur hexaflouride and ice nuclei were used to test the model. The results were in reasonable agreement with field measurements of plume positions; however, plume concentrations were underpredicted. The model was run with a Kessler warm rain parameterization to examine the characteristics of liquid condensate. Patterns of liquid water predicted by the model suggest that depletion of liquid water to the lee of the crest could be due to subsidence warming. This complicates the estimation of liquid water depletion through precipitation processes.

1. INTRODUCTION

Although measuring technology has increased the amount, variety and quality of data available from weather modification programs, there remain temporal and spatial limitations. Numerical modeling offers the opportunity to supplement the measurements, provided the models earn the confidence of the user. Modeling can also aid in operational planning and serve as a platform to test seeding strategies. Modeling has been applied to winter orographic cloud seeding programs for both operations and research. One example is described by Reynolds *et al.* (1989) who applied the GUIDE model to SCPP to estimate targeting of supercooled liquid water (LW) content and fallout during winter California orographic storms. The Clark model has been applied to the Arizona project (Bruintjes, 1992), which, like the experiment described herein, is part of the NOAA/state cooperative program. For this, the Clark model was used to predict transport and dispersion, as well as cloud parameters. The purpose of this paper is to describe the application of the Clark mesoscale model to the winter orographic weather modification activities in the Wasatch Plateau of central Utah, and to give an example of its use.

The principal goal of modeling the Utah project has been to examine the transport and diffusion of seeding material. Targeting of seeding material has been cited as a significant problem in winter orographic weather modification projects (Reynolds *et al.*, 1989; Super, 1990; Super and Huggins, 1992). This issue was listed as the second goal of the research program designed for the cooperative program (Utah Dept. of Nat. Res., 1991), which was "piggy-backed" on the Utah operational program.

2. DATA

The data applied to this modeling were collected during the Utah/NOAA Cooperative Atmospheric Modification Program run from mid-January to mid-March 1991. The experimental area was the Wasatch Plateau located in central Utah. Figure 1 shows the experimental area and the locations of some of the instrumentation. Surface meteorological parameters were monitored at the Department of Transportation (DOT) site. At this point, a dual-channel microwave radiometer (Hogg *et al.*, 1983) provided by the U.S. Bureau of Reclamation recorded vertically integrated LW amounts. A network of 5 precipitation gauges was maintained across the Plateau. Each gauge was in a sheltered location to minimize wind-induced undercatch. Wind velocity and air temperature were monitored by 3 PROBE automatic weather stations in addition to the DOT observatory. One PROBE weather station was at the High Altitude Site (HAS), one was in the entrance to Cottonwood Canyon, 3 km NE of the town of Fairview, and one was 3.3 km further up that canyon. An instrumented van sampled along a 7 km stretch called the "Skyline Drive." This is where Highway 31 parallels the west edge of the Plateau, 1 km north to 6 km south of the DOT site.

An instrumented Beechcraft King Air C-90 aircraft (N46RF) was provided by USDC/NOAA/ARC. Its configuration and scientific direction were by the NOAA/ERL/ARS in Boulder, CO. The designated flight tracks are indicated in Fig. 1 as the two S-N lines roughly on the upwind and downwind edges of the Plateau. The aircraft recorded state parameters, LW content (King/CSIRO and FSSP), ice crystal imagery (2D-C), and horizontal winds. The aircraft's position was monitored with LORAN and GPS.

Silver iodide was released by 8 valley generators established by North American Weather Consultants (hereafter NAWC) for the operational project. Ice nuclei concentrations were monitored by three acoustical counters (Langer, 1973); one in the aircraft, one at the DOT site and one in the van. For portions of the case study, sulfur hexaflouride (SF_6) was released within the mouth of Birch Creek Canyon. The SF_6 tracer gas was measured by a fast-response detector (Benner and Lamb, 1985) on the aircraft.

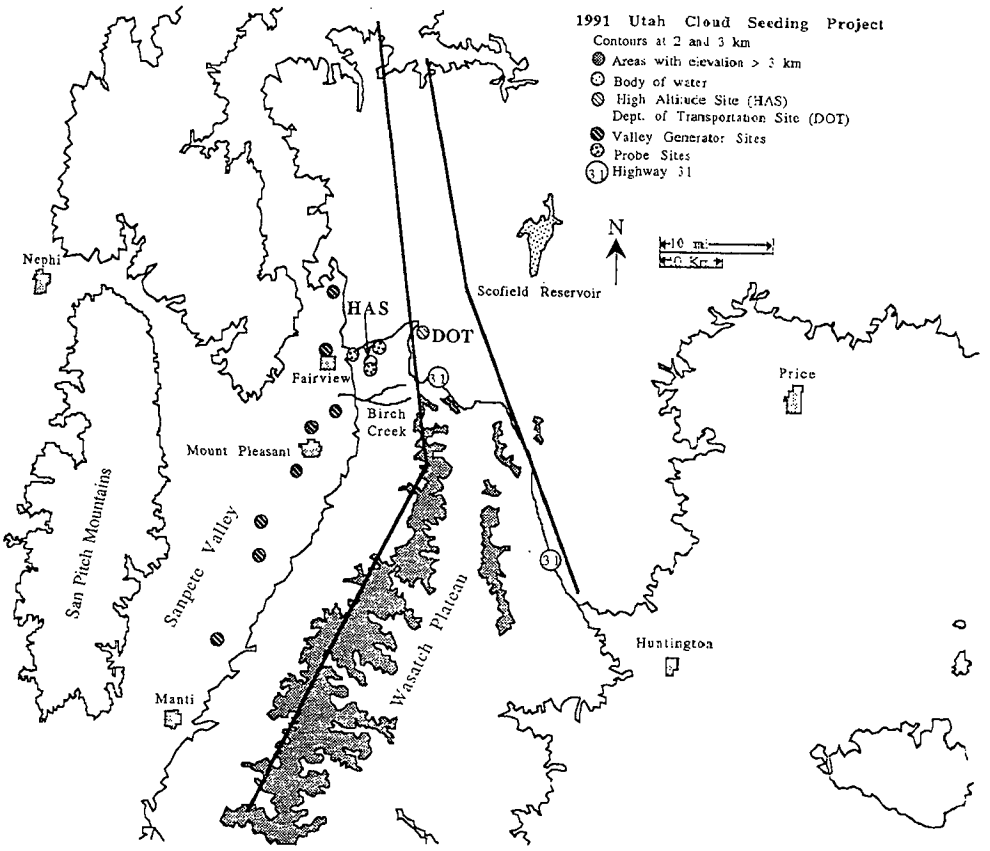

Fig. 1. The early winter 1991 Wasatch Plateau experimental area.

This was a Scientech LBF-3 instrument which has a detection limit of 10 ppt or less in normal ambient conditions.

3. MODEL DESCRIPTION AND SETUP

The three-dimensional, time dependent numerical model by Clark and associates of the National Center for Atmospheric Research (hereafter NCAR) was selected for application to the Utah program (Clark, 1977; Clark and Farley, 1984; Clark and Hall, 1991). The model is nonhydrostatic and anelastic which allows vertical acceleration but eliminates acoustic-scale waves. The model uses geo-spherical nonorthogonal coordinates with terrain following vertical coordinates such that the lowest grid points of the model are aligned with the terrain, and the top is at a constant level.

A description of the theory used to simulate the boundary layer is presented by Clark *et al.* (1994). At the surface there is an imposed stress which uses a drag law to represent surface friction. Above the surface, stress is a function of the eddy mixing coefficient, K, and the velocity field. Within the surface boundary layer, K is a function of deformation. Above the surface boundary layer, K is also a function of the eddy Prandtl number which is set to unity and the Richardson number.

The model includes a two-way interactive grid nesting procedure. This enables finer temporal and spatial resolutions to be defined within the inner domain, and a broader upwind fetch can be economically input to the model while applying the fine resolution only to the innermost areas of interest. For the applications described herein, a three-domain setup was applied. The outermost domain had a 9 km horizontal resolution; the middle, a 3 km resolution; and the innermost domain had a 1 km resolution. The vertical resolution was "stretched" with Δz being 100 m at the surface increasing to 1000 m at and above 18 km (all elevations in MSL).

3.1 Topography

The source of topography data was a file available at NCAR with a resolution of 30 sec (approx. 0.8 km) for the continental U.S. In the topography generation mode, the model determined the latitudes/longitudes for each grid point and elevations were interpolated to these points. The resulting terrain was run through a two-dimensional nine-point smoother twice to insure stability within the model. An overly rough terrain can generate noise in the model when the pressure solver is applied. Three-dimensional depictions of the three domains and their relative positions are shown in Fig. 2. The vertical scales of Fig. 2 are exaggerated. The innermost domain shows good detail of the terrain; however, the

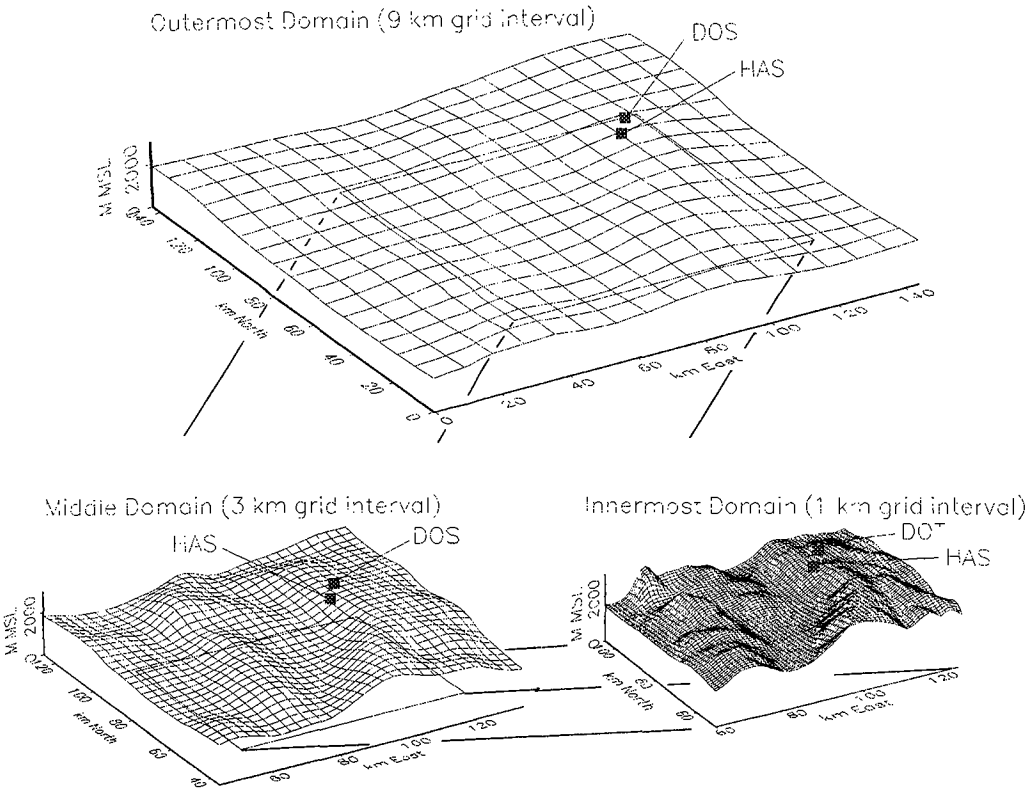

Fig. 2. Topography for the three nested models.

canyons on the west slope of the Plateau, more specifically, Birch Creek and Cottonwood canyons, are not well-defined.

Only analyses for the innermost domain are illustrated in this paper. The coordinates for these (Figs. 5, 6, 7, 9, 10 and 11) are in km from the southwest corner of the outermost domain. The coordinates for the figures illustrating airborne plume encounters (Figs. 4 and 8) are km from the DOT site. The areas and scales of the horizontal figures are identical allowing overlaying for comparative purposes.

3.2 The Initializing Sounding

The model was initialized from a single sounding. The sounding was applied homogeneously over all domains and the outermost boundary had the equation of continuity relaxed to provide zero net mass flux into the model for the variable terrain. Initially a single sounding was input to the model; however, a majority of the soundings had one or more nuances to which the model was sensitive, e.g., a shallow inversion layer or a superadiabatic zone. A composite sounding was derived by overlaying timely balloon-borne and aircraft-derived soundings. In so-doing the irregularities could be discerned. The sounding input to the model was hand-drawn and represented a somewhat smoothed profile for the time of the case study. For the 6 March case, the Ely sounding was included. This is approximately 290 km to the west of the target area. To insure computational stability, the highest available level from the composite sounding was repeated to 5 mb.

3.3 Modeling Tracer Releases

The model allows the release of tracer material from one or more locations. For the Utah application, the tracer is input to the innermost mesh as $Q = \partial M/\partial t$ (gm hr^{-1}) and is initially distributed over an entire grid bin of volume $\Delta x \Delta y \Delta z = 0.1$ km^3. The advective transport scheme of Smolarkiewicz (1983, 1984) is used in the model which requires the manipulation of a mixing ratio by mass, q, rather than a concentration (mass per volume). Following Bruintjes (1992),

$$\frac{\partial q}{\partial t} \approx \frac{\Delta q}{\Delta t} = \frac{Q}{\tilde{\rho}\Delta x \Delta y \Delta z},$$

where $\tilde{\rho}$ represents the base state of density upon which the model imposes perturbations. Since all the releases were on the surface, $\Delta z = 100$ m. The equation of conservation of tracer is

$$\tilde{\rho}\frac{dq}{dt} = \tilde{\rho}\frac{\partial q}{\partial t} + \nabla\cdot(\tilde{\rho} K \nabla q)$$

where K is the eddy mixing coefficient. For the runs described herein, the tracer releases were turned on after the model had been integrated for one hour. In the generator portion of the model, the tracer material was kept as a mixing ratio. This was converted to picograms per cubic meter (10^{-12} gm m^{-3}, hereafter

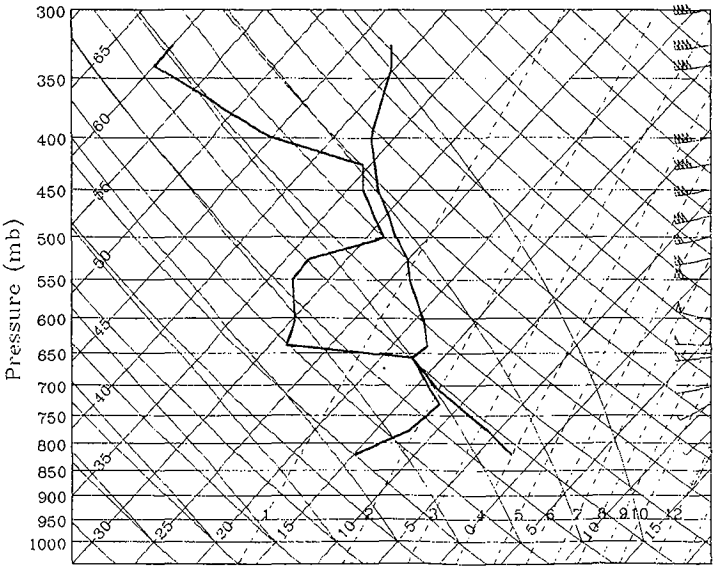

Fig. 3. Composite sounding used to initialize model for 6 March 1991.

pgm m^{-3}) in the analysis portion.

3.4 Warm Rain Parameterization

The Clark model has an option which simulates warm rain production. The term "warm rain" implies liquid condensate which can be supercooled. A modified form of the Kessler (1969) parameterization is used. A detailed description of the warm rain application within the model is given by Clark (1979). The Kessler parameterization assumes there are two forms of condensed water: cloud water and rain water. Drop-size distributions, fall velocities and conversion from cloud to rain water are calculated from empirical arguments. This so-called "bulk-parameterization" simplifies the calculation of liquid condensation by assuming a given shape or characteristic spectrum for each class of hydrometeor. The alternative is a detailed approach where the spectrum of each hydrometeor class is subdivided into many independent variables and the microphysical calculations can be formally treated. This latter approach is far more expensive in terms of computer time and memory, though probably more accurate. The ice phase option of the model was not applied to the case described in this paper.

3.5 Logistics of Running Model

The model was run on the NCAR CRAY YMP located in Boulder, CO. The model's run parameters were input by making changes to the FORTRAN code stored on the CRAY, then compiling the program. The changes were made by submission of JCL (job control language) which is used by the CRAY system to make insertions, substitutions and deletions to the code in a temporary file. Graphics output was sent to the machine of choice through the use of the UNIX rcp command and processed locally using NCARGraphics software. For each hour of simulated time, approx. 10 Mbytes of graphics were produced and approx. two hours of CRAY CPU time were required.

4. ANALYTICAL TECHNIQUES

4.1 Sulfur Hexaflouride Data

The aircraft SF_6 data used in this report were the post-season processed data provided by NAWC, whose technicians were responsible for the airborne detector. False signals, such as those induced by sudden changes in cabin pressure, were found by visual inspection of the data and flight notes. Ice nuclei concentrations resulting from co-released AgI and SF_6 can be inferred if the dilution factor for SF_6 is assumed to be the same as for AgI from collocated sources. This assumes that scavenging and sedimentation processes are negligible or similar for the two substances. Equation (2) below was used to estimate concentrations of AgI (gm m^{-3}).

$$\chi_{AgI}=1.7567X10^{-9}\frac{Q_{AgI}}{Q_{SF6}}\frac{fp}{T}. \qquad (1)$$

The source strengths of AgI and SF_6 are Q_{AgI} and Q_{SF6} (mass per time). The concentration of SF_6 is f which is expressed in ppt by volume. The ambient pressure, p, is in mb and T is °K.

4.2 Calculating Airborne AgI Plume Positions

The IN detector's response is lagged due to delays caused by plumbing and the time needed to grow acoustically-detectable crystals (≥ 20 μm). The response is also smoothed because of mixing within the cloud chamber. The response of the detector was calibrated in a series of ground tests and airborne sampling of co-released AgI and SF_6 plumes. The most precise response parameter was found to be the AgI plume entry delay determined from the time of first response. Since the flights consisted of pairs of passes in opposite directions, approximations of horizontal extent of IN could be made using pairs of plume edges.

Previous work by Super *et al.* (1988) suggests that the lag time to plume edge is a power function of the sum of IN counts for the entire plume penetration. The AgI plume edge times used in this paper are defined by the first second of seven seconds having ≥ 3 IN counts. This method was appropriate for the small concentrations typically detected by the aircraft. The power curve fit is

$$lag(\text{sec})=96.7\left(\sum cnts\right)^{0.228}-0.5. \qquad (2)$$

The range of measured lag times for small IN

sums was approximately ± 20 s, which corresponds to approximately 1.8 km flight distance. For Σ cnts < 15, the three counts in 7 s criteria could usually not be met. In this case, a coarse estimate of the mean lag for all IN detected in a given pass was used to approximate the plume position. This was found to average 89 s. For the 6 March case, Eq. (2)'s minimal sum of counts criterium was met for all aircraft passes.

5. MODELING THE 6 MARCH CASE

5.1 Weather and Data Collection

The case discussed in this paper occurred on 6 March 1991. This was a cold storm with little liquid water and no imbedded convection. On this date, a short wave passed the target area between 1730 and 1740. Preceding the wave was a small area of moisture as well as cold air advection. At the DOT site, the winds were Wly prior to frontal passage, veering to WNWly by 1900. Behind the wave there was some drying and diurnal warming. The Mount Pleasant and the 1600 Ely soundings indicated winds of less than 7 m s^{-1} below 700 mb.

At the DOT site, the wind direction trends were similar to the soundings'. During the experimental period, the DOT site's speeds were 4 to 6 m s^{-1}, declining to 2 to 4 m s^{-1} after 1930, then becoming nearly calm by midnight. At the two Cottonwood Canyon PROBE sites, both up-canyon and down-canyon winds were recorded. The down-canyon winds, presumably katabatic, occurred between approximately 0600 and 0915, and after 2115. The speeds at both sites were 3 to 4 m s^{-1} until 0425, and 0 to 2 m s^{-1} thereafter. The relative humidities and temperatures at the Cottonwood Canyon sites followed a diurnal trend with low humidities and high temperatures occurring during the daylight hours. The percent relative humidities ranged from the low 40's to the mid 80's, and the temperatures from -12.9 to -3.3°C at both sites.

For the 6 March case, the aircraft was over the experimental area from 1615 to 1915. During this time, 14 N-S passes were made, of which two were on the east track. The first nine passes were made at the minimum IFR elevation, as shown on Figs. 6, 7 and 10. Thereafter, all passes were made at a constant 3.7 km. Average temperatures and pressures at flight level ranged from -19 to -15 °C and 655 to 687 mb respectively during plume encounters.

Precipitation was recorded on the Plateau in the early morning, and during the experimental period. The DOT site received the largest amount of precipitation of the Plateau gauges, both in terms of duration and quantity.

The radiometer at the DOT site indicated a small amount of vertically integrated LW in the early morning and again after 1000 (Huggins *et al.*, 1992). The peak hourly-averaged LW depth recorded was 0.04 mm during the hour ending 1400. Satellite-derived cloud-top temperatures were between -20 and -15 °C except from 1200 to 1800 when the cloud-top temperatures ranged from -31 to -27 °C.

Defining the initial conditions for the model was not straightforward because there were two distinct sounding types. Prior to the short wave passage there was a subsidence inversion based at 650 mb. As the wave approached, this changed to lapse conditions with little variation in the profile below 650 mb. The initializing sounding was a compromise between the two regimes which had a small inversion at 650 mb. This profile is shown in Fig. 3.

5.2 Modeling the Birch Creek SF_6 Release of 6 March 1991

Sulfur Hexaflouride was released from 1605 to 1915 on 6 March at a rate of 22.7 kg hr^{-1} from the mouth of Birch Creek Canyon. Figure 4 is a composite of all airborne plume penetrations for this date. The peak SF_6 value detected was 903 ppt at 1847 on the west track. After this, there were two passes by the aircraft on the west track, during which no SF_6 was detected, presumably due to the cessation of SF_6 release. Of the 13 passes excluding the last two, the lowest peak value was 41 ppt.

If a Montana State University generator dispensing 30 gm hr^{-1} was collocated at the SF_6 site, then the range of inferred peak AgI concentrations found by the application of Eq. 1 would be $2.5X10^2$ to $5.5X10^3$ pgm m^{-3}. Applying the calibration of this generator (Super and Heimbach,1983) to the inferred AgI concentrations gives peak effective IN concentrations ranging from 150 to 3300 IN L^{-1} effective at flight-level temperatures. Use of mean SF_6 concentrations would produce smaller concentrations of IN by up to an order of magnitude (Griffith *et al.*,1992).

A 30 gm hr^{-1} AgI release from the Birch Creek surface site was modeled. Fig. 5 shows the modeled plume at 2.9 km after a 2 hr release. No contours were present on the next higher analysis level. The model predicted the general W-E transport and meander of the plume measured at higher levels by the aircraft. At the 2.9 km level there is one small element which moved to the NE. There are three west-to-east zones of higher concentrations. The westernmost is due to the proximity of the source to the vertical motion forced by the windward edge of the plateau. The others result from the vertical motion caused by gravity waves; the higher concentrations being in areas of upward motion. The surface plume (not shown) had a northward drift in the valley and lateral spreading, which was induced by low-level directional shear. Observations by the aircraft and surface wind observations suggest the plume was transported up the Birch Creek Canyon; however, the model's 1 km topography did not have enough

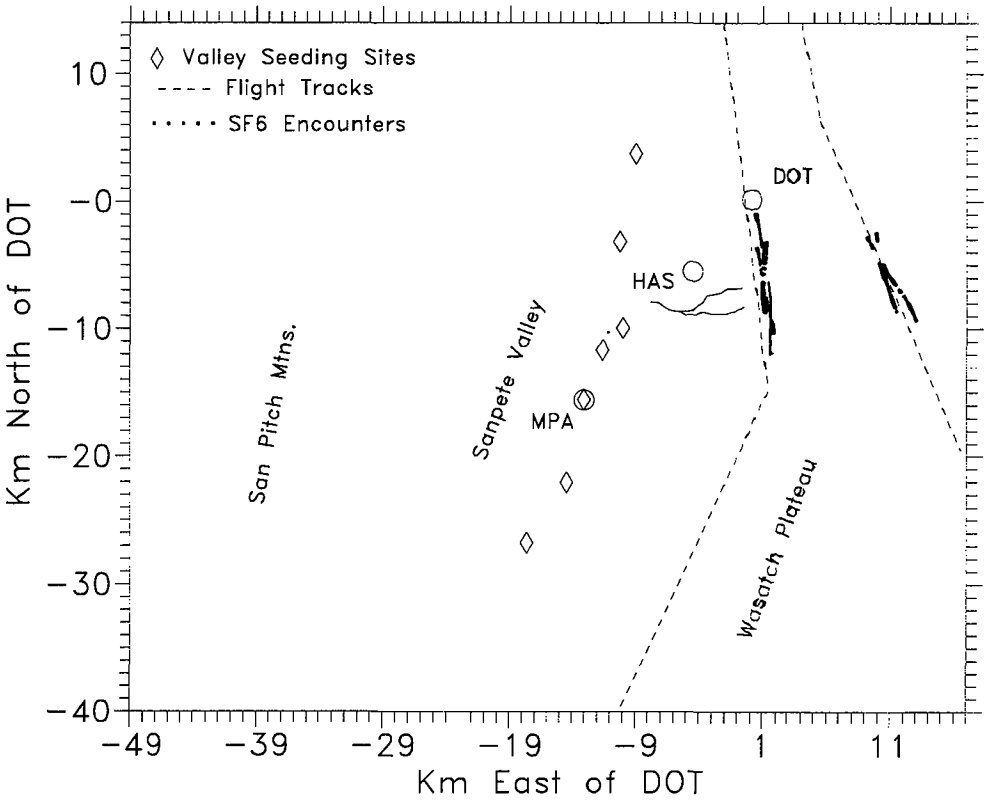

Fig. 4. Composite airborne SF_6 encounters from 6 March 1991 flight.

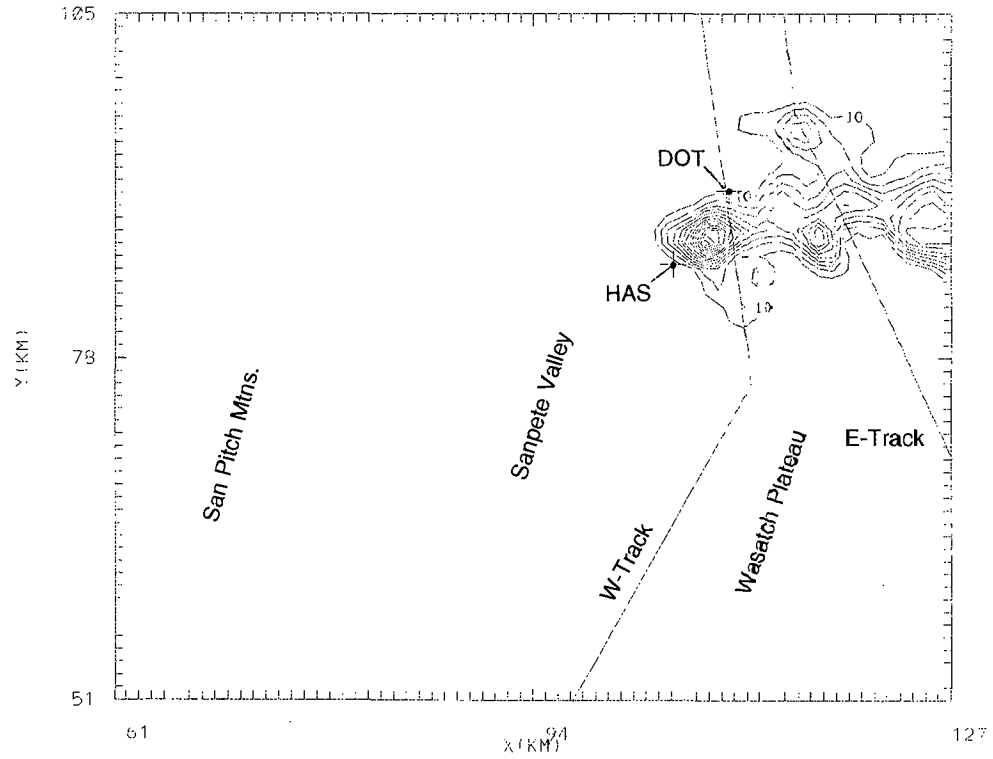

Fig. 5. Contours of modeled AgI at 2.9 km for 6 March 1991 simulated release from Birch Creek. The release time was 2 hr after an initial 1 hr integration. In this and the other figures showing AgI concentrations, the minimum contour and contour interval are 10 picograms per cubic meter (pgm m^{-3}).

resolution to mimic this situation on this day.

A S-N vertical cross section of modeled AgI through the DOT site is shown in Fig. 6 which is for the same time as Fig. 5. This figure also depicts the west flight track which has its minimum IFR elevation decrease to the north of the DOT site. The model indicates less than 10 pgm m^{-3} at minimum IFR level, predicting lower concentrations than suggested by the SF_6 monitoring. The differences may be due to the use of peak SF_6 concentrations and the initial spread of the modeled tracer material through one grid bin. The model properly predicted a rapid decrease in concentration with elevation, but more rapidly than the aircraft sampling of SF_6 suggests. Figure 7 is a S-N cross section 5 km to the west of Fig. 6. This figure demonstrates the effect of vertical motion over the Plateau. In the western cross section, the simulated AgI plume has more than double the elevation above ground level than the other; however, the minimum contour has about the same elevation MSL. Both highlight the plume's transport over lower topography of the plateau.

5.3 Valley AgI Releases for 6 March 1991

Silver Iodide was released from each of the operational valley sites on 6 March using the NAWC generators which dispensed 8 gm AgI hr^{-1}. The releases started after 1215 and ended at or before 2135. The plume edges from this flight are shown in Fig. 8. All the plume penetrations had sufficient numbers of IN to meet the criteria for edge determination. There is a preponderance of edges in the vicinity of Birch Creek Canyon. Three edges, including two on the east flight track suggest a transport through the vicinity of the DOT site. There are several edges east of Mount Pleasant. Overall, effluent from the northern 6 valley sites appears to have been detected by aircraft sampling. The total number of IN registered per plume penetration ranged from 30 to 353, with the maximum being the first pass

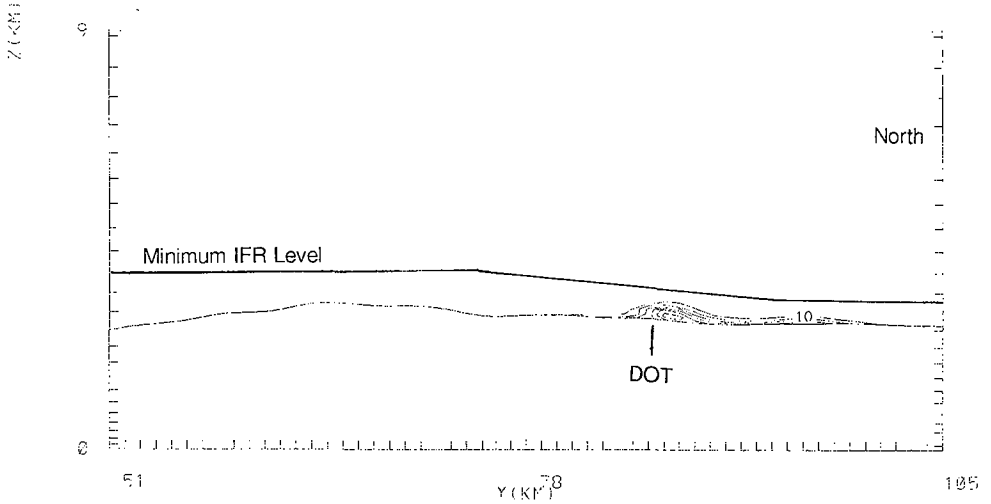

Fig. 6. North-south vertical cross section showing contours of AgI for simulated release from Birch Creek Canyon for 6 March 1991. This cross section is through the DOT site. In this and the other north - south cross sections, the minimum IFR elevation of the west flight track is drawn.

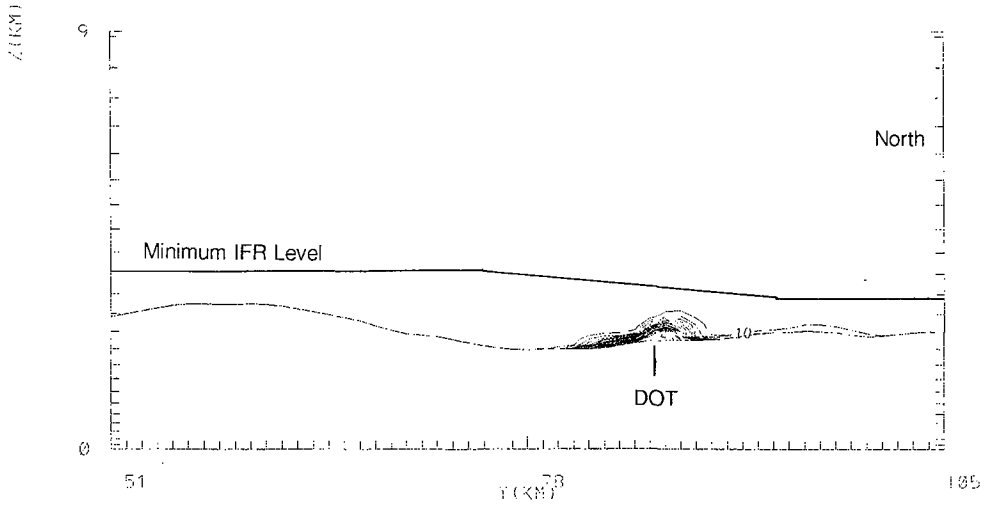

Fig. 7. Same as Fig. 6 but 5 km to west.

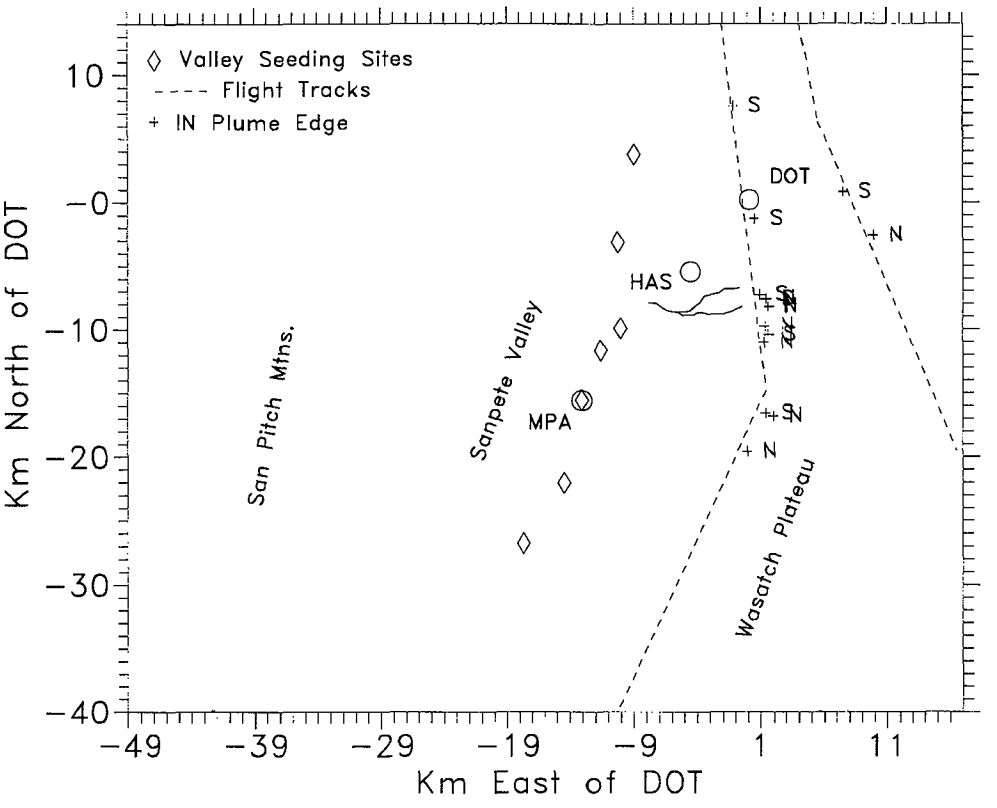

Fig. 8. Ice nuclei plume edges from flight of 6 March 1991. Crosses indicate estimated plume entry points, and "N" and "S" show the direction of flight.

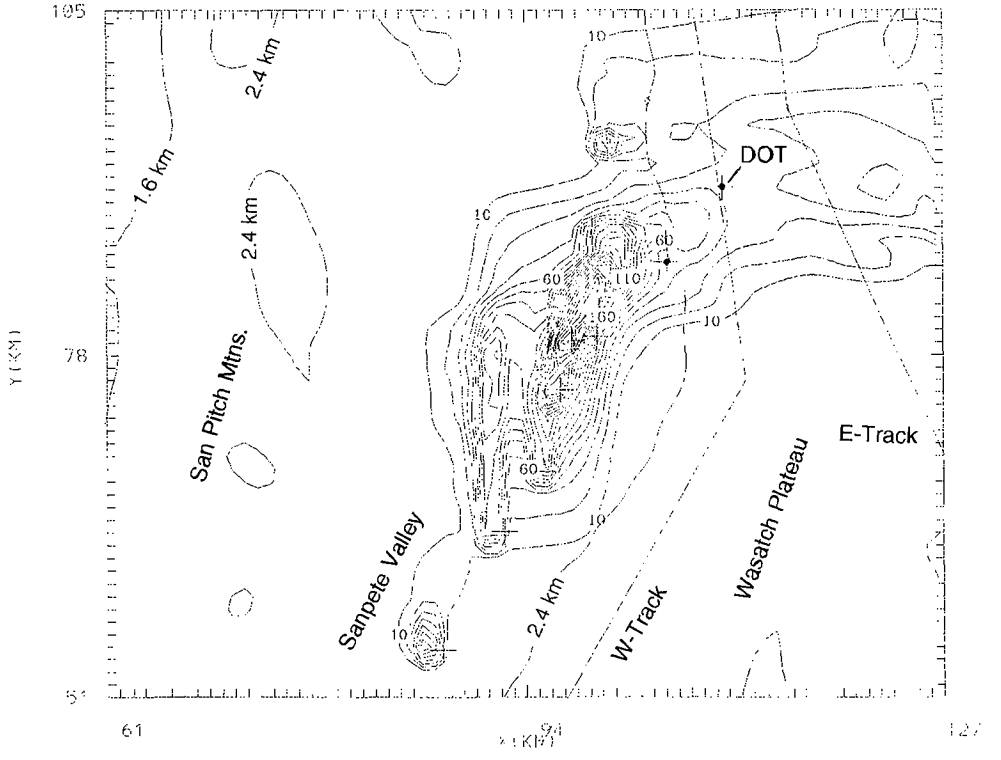

Fig. 9. Surface concentrations of AgI from simulated release of 8 gms hr^{-1} from each of eight valley sites for 6 March 1991. The contours are for 2 hr release after an initial 1 hr integration of the model. Undotted crosses indicate AgI release points.

which was farthest to the north.

A simulated release of eight gms AgI hr^{-1} from each of the 8 valley sites was modeled. The release started as the others, one hour after the initialization of the model and continued for two hours. By the end of the run, the model showed transport of AgI over the Plateau but limited to the northern portion of the experimental area, which has the lower elevation (Fig. 9). The surface plot shows a pooling of AgI in the valley and some spread to the west due to a shallow easterly flow modeled in some portions of the valley. The pooling was confirmed by surface measurements of IN taken by the van after 2100. The van sampled through Cottonwood Canyon to Fairview. No IN were detected at or above 2.0 km. Concentrations increased to 5500 L^{-1} effective at -20 C at Fairview which has an elevation of 1.8 km.

Figure 10 is a S-N vertical cross section of AgI through the DOT site. This is for the same time as Fig. 9. Ice nuclei were sampled by the van along Skyline drive from 1524 to 2036. The plume was found throughout the length of the surface traverses which were from 1 km north of the DOT site to 6 km south. This occurrence was matched by the model, but surface verification was not possible to the north. The average surface concentrations found by the van were 400 to 800 IN L^{-1}, effective at -20 C. Also, ten-minute averaged IN measurements at the DOT site ranged from several hundred to over 1500 L^{-1} during the experimental period. The model showed surface concentrations of 10 to 50 pgm m^{-3} in this area (see Fig. 10). This corresponds to 100 to 500 IN L^{-1} assuming natural draft conditions over the NAWC generator and effectiveness for -20 C (Super and Huggins, 1992). Though less than the van measurements, this is in better agreement than the elevated model results which applied IN concentrations inferred by SF_6 discussed above. The somewhat better surface results suggest that vertical transport was underestimated by the model for this case.

The underprediction is also due to the minimum dimensions of an innermost grid bin being 1. X 1. X 0.1 km^3, which forces an initial plume dilution. The aircraft traveled one grid interval in approximately 10 s, therefore a more appropriate comparative value would be an average over 10 s which would lower the maximum value of SF_6 by up to an order of magnitude. Another cause for underprediction may be caused by the model's smoothed terrain providing less topographic forcing than reality. Both of these limitations could be reduced by increasing the spatial resolution of the model; however, this requires increased computer resources.

5.4 Modeling Liquid Water for 6 March 1991 Case

The 6th of March case had cloud tops at about 3.8 km (aircraft observation) and trace icing was observed. Throughout the flight there was hazy ground contact except during a FROPA at approximately 1709 to 1730. The maximum 1 min average LW content measured by the aircraft was 0.06 gm m^{-3}.

Figure 11 shows a W-E vertical cross section of liquid cloud water (q_c) after 4 hr of model integration for the 6th. The influence of a gravity wave is indicated just east of the San Pitch Mountains, where subsidence eliminated condensation. Further to the east over the San Pete Valley, a large vertical zone of condensation occurs in the ascending air. The wave's influence continues over the Plateau, showing decreasing cloud depth and q_c several km downwind of the windward edge. Aircraft observations indicated decreasing cloud heights and clear ground contact over the eastern portions of the plateau, giving credence to the model's predictions. The clouds obscured the high elevations throughout the simulation

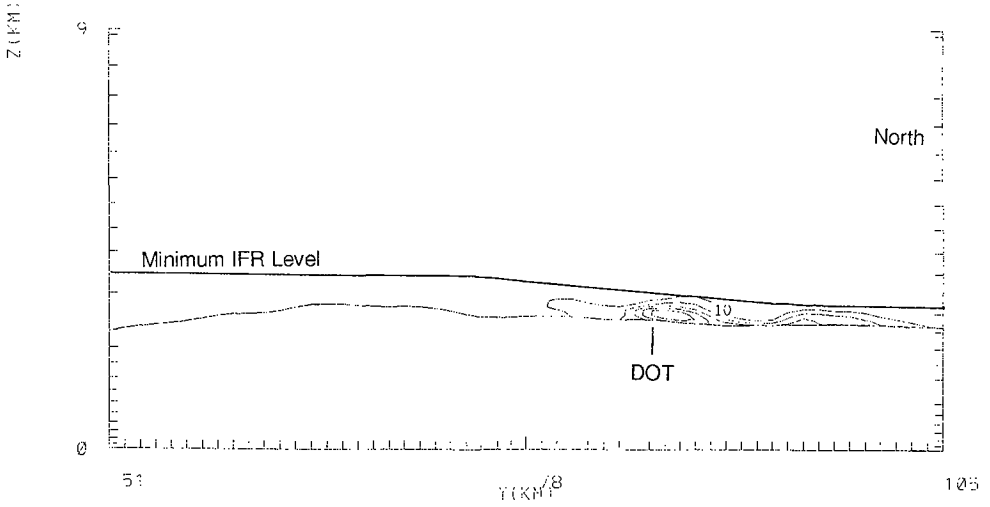

Fig. 10. North - south vertical cross section through DOT site depicting AgI concentrations resulting from 2 hr simulated release of AgI from the eight valley operational sites.

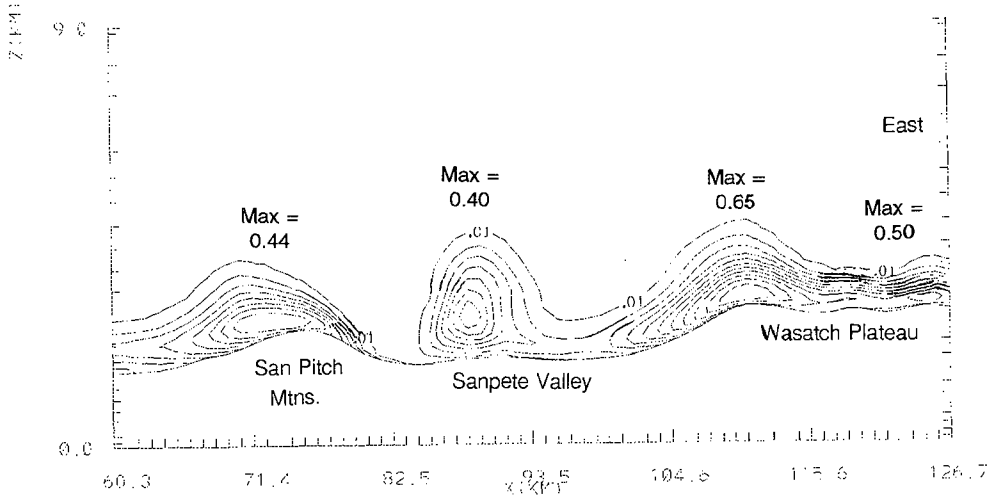

Fig. 11. West - east vertical cross section of modeled liquid water for the 6 March 1991 case after 4 hr integration. The contour interval is .06 gm kg^{-1}. A minimum contour of 0.01 gm m^{-3} is included.

and the q_c values found by the model are quite high in some areas. This may be artificially high because the ice phase was not implemented, whereas in reality, this date was one of the coldest sampled and cloud ice was observed. Over time the modeled q_c indicated a decreasing vertical thickness of condensation.

The model demonstrated a sensitivity of cloud water content to gravity waves. One of the goals of the Utah research program is to understand the effect of seeding on q_c depletion over the Plateau. Subsidence produced by gravity waves could complicate this issue.

6. DISCUSSION

The model results were in reasonable agreement with observations of plume positioning. The observed meandering of plumes, transport over lower terrain and shallow vertical dispersion were predicted by the model. The model's elevated concentrations were smaller than those inferred by SF_6 observations. This is likely for three reasons: 1) the tracer was given an instantaneous dispersal throughout one grid bin upon release; 2) the model predicted less vertical transport than reality; and 3) comparisons were done using peak SF_6 observations; however, the use of average SF_6 concentrations, though somewhat ambiguous, could not explain all the difference.

The model illustrated several points which should be considered in planning future winter orographic weather modification operations which employ surface sources.

- Seeding material can be confined to a depth of several hundred meters over the terrain.
- The horizontal and vertical positions of the release point are critical. In this study, the best release points were on the windward slopes of the barrier to take advantage of terrain-forced vertical motions.
- Pooling of seeding material can occur in the valley areas, and its transport can be guided by the character of lower terrain.

The most critical factor in ground-based targeting is placing the source in an area having positive vertical velocity near the surface. Typically, this is windward of the crest. Areas at the crest or just downwind showed small or negative vertical velocities in simulations. Valley sites can be poor locations because the vertical motion fields may not reach low enough and the valley surface winds are too poorly organized to provide consistent transport.

The use of an upwind seeding site, e.g., the San Pitch Mountains, was modeled (not illustrated in this paper) and found to have some possibility of success. An upwind release site has the advantages of providing a broader plume, earlier nucleation and opportunity for greater vertical transport. The drawbacks include targeting inconsistencies, increased lead time and dilution. It would be worthwhile to try one or more test releases from the San Pitch Mountains using a mobile source of AgI. SF_6 is not the tracer of choice for this because of the large dilutions anticipated while crossing the Sanpete Valley.

It would be useful to model transport and diffusion using a Lagrangian transport scheme. The Lagrangian treatment uses a coordinate system which follows effluent particles rather than remaining stationary. This eliminates the effect of the initial dispersion of tracer material and would give a better visual display of plume characteristics. A finer innermost mesh is needed to better simulate the effects of flow around the terrain of the experimental area. In particular, the canyons, which are important in the transport of low elevation seeding material, are not well-represented in the model. Finally, the model

is being implemented on workstation environments. Though not possible to run the model with a fine resolution on a workstation, it does offer the ability to utilize the model in a field environment, enabling an operational application in a field environment.

Acknowledgements. A. Super is acknowledged for his encouragement in the modeling effort and many fruitful discussions which helped in producing this paper. T. Clark is acknowledged for his patient and skilled tutoring in the application of the model. There are many who participated in the field work and later analysis which provided data used in this paper. C. Ogden was the operations director of the program. His organizational abilities were key to the successful conduct of the 1991 experiment. A. Huggins provided surface, sounding and satellite data summaries used in this report. G. Wilkerson provided processed SF_6 data and informative notes on the SF_6 instrumentation. J. Boatman, D. Wellman, S. Wilkerson, L. Gunter and Y. Kim of the NOAA/ERL/ARS group are cited for their part in producing an excellent data set from the 1991 flight operations. Funding for this work was through Contract No. 93-0874 between UNCA and the Utah Department of Natural Resources, Division of Water Resources as part of the Utah/NOAA Cooperative Atmospheric Modification Research Program.

7. REFERENCES

Benner, R.L. and B. Lamb, 1985: A fast response continuous analyzer for halogenated atmospheric tracers. *J. Atmos. Oceanic Tech.*, 2, 582-589.

Bruintjes, R.T., 1992: Observational and Numerical Studies of Cloud and Precipitation Development with a View to Rainfall Enhancement. Doctoral dissertation, Univ. of S. Africa. 193 pp.

Clark, T.L., 1977: A small scale dynamic model using terrain following coordinate transformation. *J. Comp. Physics*, **24**, 186-215.

_____, 1979: Numerical simulations with a three-dimensional cloud model: lateral boundary condition experiments and multi-cellular severe storm simulations. *J. Atmos. Sci.*, **36**, 2191-2215.

_____ and R.D. Farley, 1984: Severe downslope windstorm calculations in two and three spatial dimensions using anelastic interactive grid nesting: a possible mechanism for gustiness. *J. Atmos. Sci.*, **41**, 329-350.

_____ and W.D. Hall, 1991: Multi-domain simulations of the time dependent Navier Stokes equations: Benchmark error analyses of nesting procedures. *J. Comp. Phys.*, **92**, 456-481.

_____, _____ and R.M. Banta, 1994: Two- and three-dimensional simulations of the 9 January 1989 severe Boulder windstorm: Comparison with observations. [Accepted for publication in *J. Atmos. Sci.*]

Griffith, D.A., G.W. Wilkerson, W.J. Hauze and D.A. Risch, 1992: Observations of ground released sulfur hexaflouride tracer gas plumes in two winter storms. *J. Weather Mod.*, **24**, 49-65.

Hogg, D.C., F.O. Guiraud, J.B. Snider, M.T. Decker and E.R. Westwater, 1983: A steerable dual-channel microwave radiometer for measurement of water vapor and liquid in the troposphere. *J. Climate Appl. Meteor.*, **22**, 789-806.

Huggins, A.W., M.A. Wetzel and O.A. Walsh, 1992: Investigations of Winter Storms over the Wasatch Plateau During the 1991 Utah/NOAA Field Program. Final Report for the Utah Dept. of Nat. Res. Desert Research Institute, Reno Nev. 252 pp.

Kessler, E., 1969: On the distribution and continuity of water substance in atmospheric circulations. *Meteor. Monogr.*, **No. 32**, Amer. Meteor. Soc. 84 pp.

Langer, G., 1973: Evaluation of NCAR ice nuclei counter. Part I: Basic operations. *J. Appl. Meteor.*, **10**, 1000-1011.

Reynolds, D.A., J.A. Humphries and R.H. Stone, 1989: Evaluation of a 2-month cooperative ground-based silver iodide seeding program. *J. Weather Mod.*, **21**, 14-28.

Smolarkiewicz, P.K., 1983: A simple positive definite advection scheme with small implicit diffusion. *Mon. Wea. Rev.*, **111**, 479-486.

Smolarkiewicz, P.K., 1984: A fully multidimensional definite advection transport algorithm with small implicit diffusion. *J. Comp. Phys.*, **54**, 325-362.

Super, A.B., 1990: Winter orographic cloud seeding status in the intermountain west. *J. Weather Mod.*, **22**, 106-116.

_____ and J.A. Heimbach, Jr., 1983: Evaluation of the Bridger Range winter cloud seeding experiment using control gauges. *J. Climate Appl. Meteor.*, **22**, 1989-2011.

_____ and A.W. Huggins, 1992: Investigations of the targeting of ground-released silver iodide in Utah. Part II: Aircraft observations. *J. Weather Mod.*, **24**, 35-48.

_____, B.A. Boe, E.W. Holroyd, III, and J.A. Heimbach, Jr., 1988: Microphysical effects of wintertime cloud seeding with silver iodide over the Rocky Mountains. Part I: Experimental design and Instrumentation. *J. Appl. Meteor.*, **27**, 1145-1151.

Utah Department of Natural Resources, Division of Water Resources, 1991: 1991 Field Operations Plan, Utah/NOAA Cooperative Atmospheric Modification Research Program. Salt Lake City, 27 pp.